

Momentum density and Compton profile of the inhomogeneous interacting electron system. II. Application to atoms

L. Lam

*Department of Physics, City College, City University of New York, New York, New York 10031**
and Department of Physics, Columbia University, New York, New York 10027

P. M. Platzman

Bell Laboratories, Murray Hill, New Jersey 07974

(Received 31 December 1973)

The locally averaged method which treats an inhomogeneous interacting electron gas as an average over many systems with locally uniform densities is applied to calculate the momentum density and Compton profile of atomic argon and krypton. The results show good agreement with experiment and marked improvement over simple Thomas-Fermi calculations.

I. INTRODUCTION

In the past few years^{1,2} there has been renewed interest in the momentum density and the associated Compton profiles of a variety of electronic systems. The Compton profile $J(q)$ (see the previous paper hereafter called I) can be measured directly and is related to the momentum density $N_{\vec{p}}$ by

$$J(q) = \int dp_x dp_y [N_{\vec{p}}]_{p_z=q}. \quad (1)$$

In all real electronic systems (atoms, molecules, solids, etc.) both spatial inhomogeneity and the electronic Coulomb correlations are present and are reflected in the function $N_{\vec{p}}$. A general method enabling one, in principle, to calculate $N_{\vec{p}}$ taking these two factors fully into account was formulated in I. This general approach is based on Feynman's theorem and the Hohenberg-Kohn theory of the inhomogeneous electron gas. In this paper one of the special cases, *viz.*, the locally averaged method, introduced in Sec. III B of I will be applied to atomic argon and krypton.

Atoms are the simplest finite systems containing a number of interacting electrons. The spherical symmetry of the nuclear potential $V(\vec{r})$, which leads to the spatial inhomogeneities makes atoms easier to handle theoretically than other finite systems, e.g., molecules. In addition to this, the core electrons of many other complicated systems such as solids are atomic or ionic in character so that an understanding of atoms is an essential first step in our interpretation of data taken in solids. In order to find the Compton profile of the conduction electrons in metals, for example, it is necessary to know the core part first and subtract it from the total profile.³ It is a good approximation to assume that the core electrons have wave functions which are essentially unchanged from the corresponding atomic wave functions. The Compton profiles of these systems are typically obtained utilizing

Hartree-Fock atomic wave functions. For practical reasons it would be of interest to find a simpler way to accurately determine the atomic Compton profiles and thus ease the job of subtraction in solids.

At the present time the Compton spectrum of the three lightest noble elements, helium, argon, and krypton are the only ones to have been measured.⁴ With the perfection of the γ -ray technique this list will soon be lengthened. For the three elements mentioned above their Compton profiles have been calculated either by Fourier transforming the self-consistent wave functions⁴ or by using the Thomas-Fermi approximation.⁵ As we will show below (Sec. III) the Thomas-Fermi method is far from adequate in explaining the Compton profiles. On the other hand, for high- Z atoms, where Z is the atomic number, wave functions must include relativistic effects properly and they become increasingly difficult to obtain. With these facts in mind the locally averaged method of I is presented here as an alternative to the self-consistent wave-function calculations. Its merit and accuracy will be reviewed in Sec. II.

Section III contains the numerical calculations for atomic argon and krypton using the above method together with the Thomas-Fermi results for comparison purposes. General discussions are then presented in Sec. IV.

II. THEORY

The idea of treating a system of inhomogeneous interacting Fermi particles as locally homogeneous and in equilibrium dates back to the original Thomas-Fermi approximation.⁶ Since then different kinds of variations of this scheme have received considerable attention.^{5,7,8}

The Fermi-Thomas method always works best when the gradients of the density are small. However, the actual magnitude of the corrections to

such a scheme depend on the explicit quantity which is being calculated. In I it was pointed out that the locally-averaged-density method as applied to a calculation of the momentum density might have an extremely wide range of validity, i. e., be quite insensitive to gradients. This method approximates the momentum density $N_{\vec{p}}$ by

$$N_{\vec{p}} = \int N_{\vec{p}}^0(n(\vec{r})) n(\vec{r}) d\vec{r}. \quad (2)$$

Here $n(\vec{r})$ is the local charge density and $N_{\vec{p}}^0(n(\vec{r}))$ is the momentum density of a homogeneous interacting electron gas of constant density $n(\vec{r})$. The leading corrections to Eq. (2) have been evaluated in I. Combining (1) and (2), we arrive at a simple expression for the Compton profile

$$J(q) = \int J_n^0(q) n(\vec{r}) d\vec{r}. \quad (3)$$

Here $J_n^0(q)$ is the Compton profile of the homogeneous gas at a density n .

The Thomas-Fermi approximation results if in (3) we replace $J_n^0(q)$ by the free-electron parabolic profile and $n(\vec{r})$ by $n^{\text{TF}}(\vec{r})$ where

$$n^{\text{TF}}(\vec{r}) = (32/9\pi^3) Z^2 [\Phi(x)/x]^{3/2}. \quad (4)$$

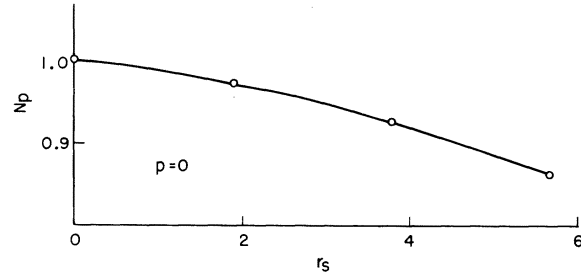
In atomic units ($\hbar = m = e^2 = 1$)

$$x \equiv 2(4/3\pi)^{2/3} Z^{1/3} r, \quad (5)$$

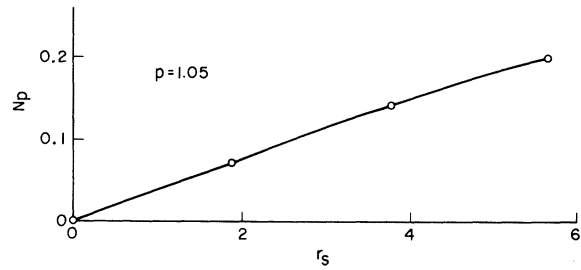
and $\Phi(x)$ is a function satisfying the Thomas-Fermi equation

TABLE I. Compton profiles of Ar.

| q | WF | Expt. | LAM | TS | HF | TF |
|------|-------|-------|-------|-------|-------|-------|
| 0.0 | 5.052 | 5.058 | 5.378 | 5.607 | 5.626 | 8.245 |
| 0.1 | 5.028 | 5.022 | 5.299 | 5.462 | 5.433 | 7.106 |
| 0.2 | 4.950 | 4.917 | 5.044 | 5.123 | 5.119 | 5.744 |
| 0.3 | 4.812 | 4.749 | 4.727 | 4.770 | 4.781 | 4.885 |
| 0.4 | 4.608 | 4.526 | 4.405 | 4.423 | 4.445 | 4.263 |
| 0.5 | 4.369 | 4.259 | 4.090 | 4.091 | 4.120 | 3.782 |
| 0.6 | 4.028 | 3.960 | 3.787 | 3.776 | 3.808 | 3.394 |
| 0.7 | 3.690 | 3.643 | 3.499 | 3.478 | 3.513 | 3.072 |
| 0.8 | 3.328 | 3.319 | 3.226 | 3.199 | 3.232 | 2.800 |
| 0.9 | 2.982 | 3.000 | 2.970 | 2.937 | 2.967 | 2.567 |
| 1.0 | 2.658 | 2.697 | 2.729 | 2.692 | 2.720 | 2.363 |
| 1.2 | 2.108 | 2.164 | 2.295 | 2.253 | 2.275 | 2.027 |
| 1.4 | 1.701 | 1.753 | 1.920 | 1.876 | 1.890 | 1.759 |
| 1.6 | 1.417 | 1.461 | 1.601 | 1.557 | 1.564 | 1.542 |
| 1.8 | 1.221 | 1.264 | 1.336 | 1.294 | 1.296 | 1.362 |
| 2.0 | 1.084 | 1.129 | 1.122 | 1.084 | 1.080 | 1.211 |
| 2.5 | 0.873 | 0.924 | 0.812 | 0.795 | 0.795 | 0.923 |
| 3.0 | 0.736 | 0.744 | 0.685 | 0.678 | 0.681 | 0.721 |
| 3.5 | 0.621 | 0.634 | 0.591 | 0.587 | 0.591 | 0.575 |
| 4.0 | 0.520 | 0.534 | 0.512 | 0.509 | 0.512 | 0.465 |
| 5.0 | 0.351 | 0.366 | 0.379 | 0.376 | 0.380 | 0.316 |
| 6.0 | 0.249 | 0.260 | 0.274 | 0.271 | 0.274 | 0.222 |
| 7.0 | 0.177 | 0.181 | 0.192 | 0.189 | 0.191 | 0.161 |
| 8.0 | 0.130 | 0.137 | 0.131 | 0.129 | 0.129 | 0.119 |
| 9.0 | 0.098 | 0.104 | 0.089 | 0.088 | 0.088 | 0.090 |
| 10.0 | 0.075 | 0.078 | 0.064 | 0.063 | 0.063 | 0.069 |
| 15.0 | 0.025 | 0.025 | 0.026 | 0.025 | 0.025 | 0.022 |



(a)



(b)

FIG. 1. Momentum density $N_{\vec{p}}$ as a function of r_s for fixed p . (a) $p=0$, (b) $p=1.05$ ($p_F=1$). Data from Ref. 11.

$$\frac{d^2\Phi(x)}{dx^2} = x^{-1/2} [\Phi(x)]^{3/2}. \quad (6)$$

This function $\Phi(x)$ can be approximated by⁹

$$\Phi(x) = [(1 + 1.81061x^{1/2} + 0.60112x)/(1 + 1.81061x^{1/2} + 1.39515x + 0.77112x^{3/2} + 0.21465x^2 + 0.04793x^{5/2})]^2. \quad (7)$$

These results will be useful in the numerical calculations presented in Sec. III.

III. CALCULATIONS

In Table I we give the calculated Compton profiles of argon ($Z=18$). The experimental results⁴ (Expt) and wave-function calculations⁴ (WF) are also listed for comparison. The last column (TF) in the table is the Thomas-Fermi calculation using Eqs. (4)–(7). The fourth column, marked LAM (locally averaged method) in the table gives the results using (3) with a charge density obtained from Tong and Sham (TS).¹⁰ The Tong-Sham $n(\vec{r})$ is calculated by the Kohn-Sham self-consistent scheme.¹²

The momentum density of a homogeneous gas may be considered to be a function of two independent variables, i. e., the momentum p and the gas density n , or equivalently, p and r_s . The quantity

r_s in atomic units is $(4\pi n/3)^{-1/3}$. In Fig. 1 we show the typical variation of N_p^0 with r_s (the RPA result) for two values of p (the Fermi momentum $p_F=1$).¹¹ For typical atoms the relevant r_s falls within the range $0 < r_s < 2.5$ (see Fig. 4). From Fig. 1 we see that for this domain of r_s , to a first approximation we may write

$$N_p(r_s) = A_p r_s + B_p \quad (8)$$

for all p . In our calculations the linear term in Eq. (8) is fixed by the two points $r_s=0$ and $r_s=1.9$. It follows from (1) that the Compton profile has a similar linear dependence on r_s .

The fifth column (TS) is calculated utilizing the same Tong and Sham¹⁰ charge density as before, but instead of using RPA expressions for the homogeneous gas we have used the free-electron Fermi distribution. The sixth column (HF) uses charge densities from Hartree-Fock calculations¹³ and the same RPA local Compton profiles as that in the LAM column.

As shown in Table I, the Thomas-Fermi results are not in good agreement with experiment. Comparisons between the columns LAM, TS, and HF show that the use of various $n(\vec{r})$ and $J_n^0(q)$ in (3) does make a difference. While it is clear that the direct wave function results give the best agreement, it is also clear that the LAM calculations

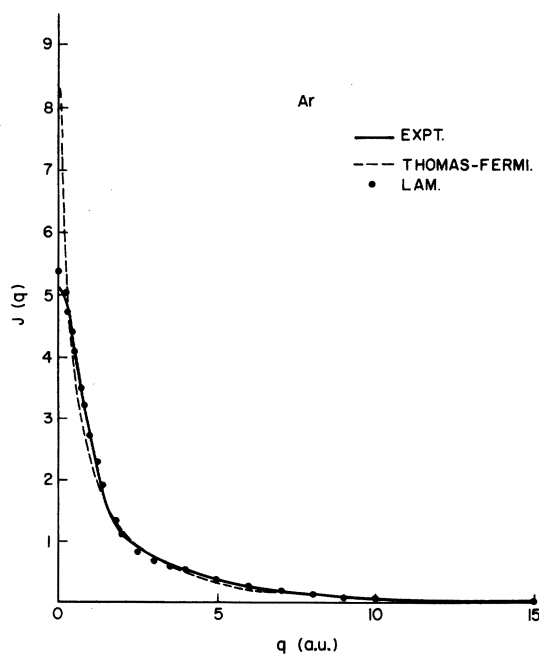


FIG. 2. Compton profiles of Ar. Solid line, experiment from Ref. 4. Dashed line, calculated Thomas-Fermi results. Dots, LAM calculation (see Sec. III).

TABLE II. Compton profiles of Kr.

| q | WF | Expt. | LAM | TS | TF |
|------|-------|-------|-------|-------|--------|
| 0.0 | 7.228 | 7.205 | 7.240 | 7.448 | 10.363 |
| 0.1 | 7.194 | 7.152 | 7.182 | 7.378 | 9.797 |
| 0.2 | 7.085 | 7.022 | 7.013 | 7.168 | 8.417 |
| 0.3 | 6.888 | 6.767 | 6.735 | 6.819 | 7.395 |
| 0.4 | 6.595 | 6.459 | 6.360 | 6.387 | 6.634 |
| 0.5 | 6.216 | 6.098 | 5.968 | 5.971 | 6.030 |
| 0.6 | 5.776 | 5.701 | 5.590 | 5.576 | 5.533 |
| 0.7 | 5.309 | 5.289 | 5.230 | 5.205 | 5.112 |
| 0.8 | 4.848 | 4.880 | 4.891 | 4.857 | 4.750 |
| 0.9 | 4.420 | 4.491 | 4.574 | 4.534 | 4.433 |
| 1.0 | 4.039 | 4.133 | 4.277 | 4.233 | 4.152 |
| 1.2 | 3.441 | 3.540 | 3.747 | 3.698 | 3.677 |
| 1.4 | 3.037 | 3.122 | 3.299 | 3.249 | 3.288 |
| 1.6 | 2.769 | 2.850 | 2.927 | 2.881 | 2.962 |
| 1.8 | 2.583 | 2.670 | 2.629 | 2.589 | 2.686 |
| 2.0 | 2.441 | 2.533 | 2.399 | 2.368 | 2.448 |
| 2.5 | 2.144 | 2.219 | 2.024 | 2.010 | 1.977 |
| 3.0 | 1.857 | 1.898 | 1.764 | 1.756 | 1.628 |
| 3.5 | 1.578 | 1.597 | 1.551 | 1.545 | 1.362 |
| 4.0 | 1.326 | 1.338 | 1.343 | 1.335 | 1.152 |
| 5.0 | 0.934 | 0.937 | 1.008 | 1.000 | 0.848 |
| 6.0 | 0.678 | 0.683 | 0.741 | 0.734 | 0.642 |
| 7.0 | 0.512 | 0.522 | 0.534 | 0.523 | 0.497 |
| 8.0 | 0.400 | 0.399 | 0.384 | 0.379 | 0.392 |
| 9.0 | 0.319 | 0.316 | 0.294 | 0.290 | 0.313 |
| 10.0 | 0.259 | 0.254 | 0.243 | 0.241 | 0.253 |
| 15.0 | 0.104 | 0.095 | 0.111 | 0.110 | 0.100 |
| 20.0 | 0.049 | 0.044 | 0.047 | 0.046 | 0.047 |
| 25.0 | 0.026 | 0.022 | 0.023 | 0.022 | 0.024 |
| 30.0 | 0.015 | 0.009 | 0.014 | 0.014 | 0.014 |

are also quite accurate. In Fig. 2 the results of LAM and TF are plotted together with the experimental data.

In Table II the calculated Compton profiles for krypton ($Z=36$) are presented. Each column in the table has the same meaning as its counterpart in Table I. The same conclusions about argon can also be drawn here. The results of LAM, TF, and experiment⁴ from Table II are plotted in Fig. 3. In this case the agreement between LAM and experiment at the origin is much closer than in the case of argon.

The above conclusions remain valid even when the revised experimental data of Eisenberger and Reed¹⁴ are used instead of the data⁴ quoted here.

IV. DISCUSSION

The agreement between the LAM calculations and experiment for argon and krypton give us some confidence that LAM works quite well in atoms. This coincides with the conclusions of Park and Rotenberg,¹⁵ who used the same kind of approximation to calculate the atomic scattering factors. In both cases, the LAM results show marked improvement over the Thomas-Fermi results and are close to the wave-function calculations.

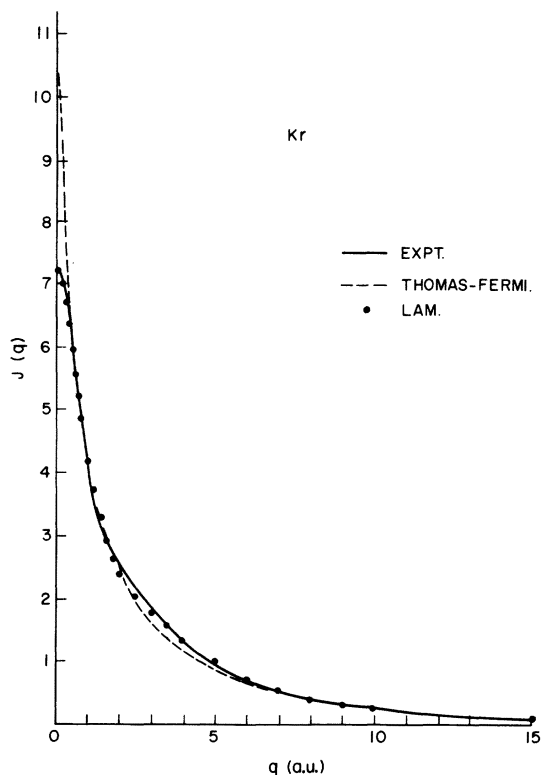


FIG. 3. Compton profiles of Kr. Symbols the same as in Fig. 2.

As we have already pointed out the validity of LAM is closely tied to the requirement that r_s vary slowly in space. In Fig. 4 we plot the Tong-Sham $n(\vec{r})$ ¹⁰ and the corresponding r_s values for Kr. In this case we see *a posteriori* that r_s does vary smoothly. In fact a similar result holds for Ar.

There is another point worth making. Within the LAM, $J(q)$ for each q , [Eq. (3)] is an integral

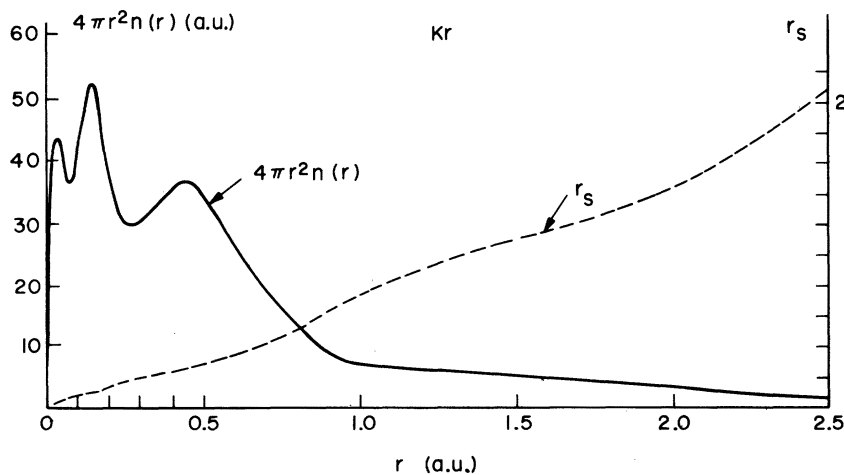


FIG. 4. Spatial charge density, $4\pi r^2 n(r)$ and the corresponding r_s for Kr. [$n(r)$ from Ref. 10].

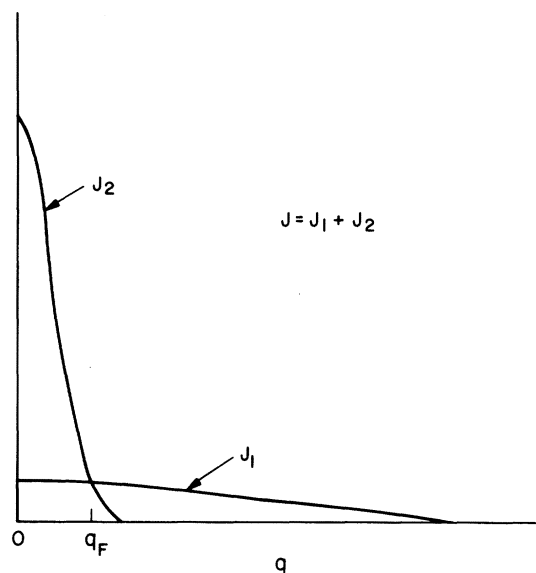


FIG. 5. Schematic plot of the two contributions to the Compton profile of atom. J_1 is from electrons near the nucleus. J_2 is from outer electrons in the atom.

over all space. However, it is clear that for different q 's $J(q)$ is in fact determined by the contributions from different space regions. For example, near $q=0$, the space integral in (3) is dominated by the contribution from the region of the atom where r_s is relatively high (low density). This may be made clearer by separating the integral in Eq. (3) into two parts:

$$J(q) = J_1(q) + J_2(q), \tag{9}$$

where

$$J_1(q) \equiv \int_0^R J_n^0(q) n(\vec{r}) d\vec{r} \tag{10}$$

and

$$J_2(q) \equiv \int_R^\infty J_n^0(q) n(\vec{r}) d\vec{r}. \tag{11}$$

R is an arbitrary value of r which crudely divides the wiggling from the smooth part of $r^2n(r)$. For example, in Fig. 4 we may choose $R \sim 0.8$ a.u. The general shape and size of J_1 and J_2 is sketched in Fig. 5. The point q_F in Fig. 5 is roughly given by $q_F = 1.92/r_s(R)$, the Fermi momentum corresponding to r_s at $r=R$.

These simple considerations indicate that the Compton profile of any atom may be roughly separated into two curves. The sharpest one, J_2 , comes from the outer electrons where the density changes rather smoothly and is expected to be given accurately by the LAM formula, Eq. (11). Since the integral under $J(q)$ is equal to the total number of electrons N , the flatter spectrum J_1 has an area which is determined by

$$\int_0^\infty J_1(q) dq = \int_0^\infty J(q) dq - \int_0^\infty J_2(q) dq \quad (12)$$

$$= \frac{N}{2} - \int_0^\infty J_2(q) dq. \quad (13)$$

J_1 as defined by Eq. (10) does satisfy this sum rule. Thus if we have a good J_2 the integral sum rule restricts the form of J_1 and tells us that at

least the average properties of J are correct.

The calculations shown in Sec. III indicate that an accurate $n(\vec{r})$ and $J_n^0(q)$ are essential to the success of the locally averaged method. This reduces its usefulness as a practical means to calculate the Compton profiles of core electrons in solids since $n(\vec{r})$ is not known before a detailed calculation is carried out. Another complication is the uncertainty of whether $n(\vec{r})$ in (3) can be taken as that part of the core electrons only without including conduction electrons. On the other hand, for atoms $n(\vec{r})$ may be inferred from x-ray diffraction experiments and the locally averaged method may be appropriate. It remains to be seen how well the method can be applied to other electronic systems, e.g., molecules.

ACKNOWLEDGMENTS

One of us (L. L.) would like to thank B. Y. Tong for sending his numerical results on atoms and Bell Laboratories, Murray Hill, at which the major part of this work was carried out, for hospitality and support. We would also like to thank P. Eisenberger, K. C. Pandey, and W. A. Reed for many interesting and informative discussions.

*Work at City College supported in part by O. N. R. and A. R. O. D.

¹L. Lam and P. M. Platzman, preceding paper, Phys. Rev. B **9**, 5122 (1974).

²M. Cooper, Adv. Phys. **20**, 453 (1971).

³P. Eisenberger, L. Lam, P. M. Platzman, and P. H. Schmidt, Phys. Rev. B **6**, 3671 (1972).

⁴P. Eisenberger and W. Reed, Phys. Rev. A **5**, 2085 (1972).

⁵N. H. March, Adv. Phys. **21**, 1 (1957).

⁶L. H. Thomas, Proc. Camb. Philos. Soc. **23**, 542 (1927); E. Fermi, Z. Phys. **48**, 73 (1928).

⁷L. Lam, M. S. thesis (University of British Columbia,

1968) (unpublished); D. McMillin, P. Bhargava, L. Lam, and E. W. Vogt, Can. J. Phys. **46**, 1141 (1968).

⁸P. C. Hohenberg and W. Kohn, Phys. Rev. **136**, B864 (1964) and references quoted therein.

⁹J. C. Mason, Proc. R. Soc. Lond. **84**, 357 (1964).

¹⁰B. Y. Tong and L. J. Sham, Phys. Rev. **144**, 1 (1966).

¹¹E. Daniel and S. H. Vosko, Phys. Rev. **120**, 2041 (1960).

¹²W. Kohn and L. J. Sham, Phys. Rev. **140**, A1133 (1965).

¹³R. D. Cowan, A. C. Larson, D. Liberman, J. B. Mann, and J. Waber, Phys. Rev. **144**, 5 (1966).

¹⁴P. Eisenberger and W. Reed (unpublished).

¹⁵D. E. Parks and M. Rotenberg, Phys. Rev. A **5**, 521 (1972).